Quantitatively Measured Anatomic Location and Volume of Optic Disc Drusen: An Enhanced Depth Imaging Optical Coherence Tomography Study

Malmqvist, Lasse; Lindberg, Anne-Sofie Wessel; Dahl, Vedrana Andersen; Jørgensen, Thomas Martini; Hamann, Steffen

Published in:
Investigative Ophthalmology & Visual Science

Link to article, DOI:
10.1167/iovs.17-21608

Publication date:
2017

Document Version
Publisher's PDF, also known as Version of record

Quantitatively Measured Anatomic Location and Volume of Optic Disc Drusen: An Enhanced Depth Imaging Optical Coherence Tomography Study

Lasse Malmqvist,[1] Anne-Sofie Wessel Lindberg,[2] Vedrana Andersen Dahl,[2] Thomas Martini Jørgensen,[2] and Steffen Hamann[1]

[1]Department of Ophthalmology, Rigshospitalet, University of Copenhagen, Glostrup, Denmark
[2]Department of Applied Mathematics and Computer Science, Technical University of Denmark, Lyngby, Denmark

Correspondence: Lasse Malmqvist, Department of Ophthalmology, Rigshospitalet, Nordre Ringvej 57, 2600 Glostrup, Denmark; lasse.malmqvist.larsen.01@regionh.dk.

Submitted: February 2, 2017
Accepted: March 29, 2017

Citation: Malmqvist L, Lindberg A-SW, Dahl VA, Jørgensen TM, Hamann S. Quantitatively measured anatomic location and volume of optic disc drusen: an enhanced depth imaging optical coherence tomography study. *Invest Ophthalmol Vis Sci*. 2017;58:2491–2497. DOI:10.1167/iovs.17-21608

Purpose. Optic disc drusen (ODD) are found in up to 2.4% of the population and are known to cause visual field defects. The purpose of the current study was to investigate how quantitatively estimated volume and anatomic location of ODD influence optic nerve function.

Methods. Anatomic location, volume of ODD, and peripapillary retinal nerve fiber layer and macular ganglion cell layer thickness were assessed in 37 ODD patients using enhanced depth imaging optical coherence tomography. Volume of ODD was calculated by manual segmentation of ODD in 97 B-scans per eye. Anatomic characteristics were compared with optic nerve function using automated perimetric mean deviation (MD) and multifocal visual evoked potentials.

Results. Increased age ($P = 0.015$); larger ODD volume ($P = 0.002$); and more superficial anatomic ODD location ($P = 0.007$) were found in patients with ODD visible by ophthalmoscopy compared to patients with buried ODD. In a multivariate analysis, a worsening of MD was significantly associated with larger ODD volume ($P < 0.0001$). No association was found between MD and weighted anatomic location, age, and visibility by ophthalmoscopy. Decreased ganglion cell layer thickness was significantly associated with worse MD ($P = 0.025$) and had a higher effect on MD when compared to retinal nerve fiber layer thickness.

Conclusions. Large ODD volume is associated with optic nerve dysfunction. The worse visual field defects associated with visible ODD should only be ascribed to larger ODD volume and not to a more superficial anatomic ODD location.

Keywords: optic disc drusen, optic nerve head drusen, 3D segmentation, visual field defects

Optic disc drusen (ODD) are bodies of extruded axonal material located in the optic nerve head.[1] They are found in up to 2.4% of the population[2] and are known to cause visual field defects,[3,4] and even complete vision loss due to complications.[5,6]

Diagnosis and classification of ODD has historically been based mainly on ophthalmoscopy. With the development of new imaging techniques, the diagnosis by ophthalmoscopy is today normally confirmed by B-scan ultrasound or optical coherence tomography (OCT).[7] However, the most frequently used classification of ODD is still based on ophthalmoscopy using none of the emerging imaging techniques. In the classification, ODD that are visible on ophthalmoscopy are termed superficial while ODD only visible by B-scan ultrasound or OCT are termed buried. Several studies have found significantly larger decreases in retinal nerve fiber layer (RNFL) thickness and automated perimetric mean deviation (MD) in patients with visible ODD when compared to patients with buried ODD.[8–11] The morphologic causes for these findings are unclear, as the ODD visibility on ophthalmoscopy might be dependent on several factors such as age, ODD volume, anatomic location of ODD, and optic nerve head anatomy.

The introduction of enhanced depth imaging OCT (EDI-OCT) has made it possible to quantify ODD anatomically.[12,13] The technique thereby enables us to decide to which degree ODD volume and anatomic location influence optic nerve function, which could be of importance for the pathophysiologic understanding of the condition.

A quantitative measure of ODD volume has only been described in a single case series,[12] while a quantitative measure of ODD location in the optic nerve head, to the best of our knowledge, never has been described. In this study, we developed a new method based on a three-dimensional (3D) analysis of the optic nerve head and semiautomatic graph-based detection of Bruch's membrane to calculate the height difference from the center of ODD mass to the defined reference surface.

The aim of this study was to investigate how volume and anatomic location of ODD influence optic nerve function using automated perimetry and multifocal visual evoked potentials (mfVEP). By including ODD visibility by ophthalmoscopy in the analysis, we assessed whether our quantitative measures were better predictors of optic nerve dysfunction than the qualitative often used classification using ODD visibility. Furthermore, we

investigated whether RNFL and macular ganglion cell layer (GCL) thickness work as anatomic correlates to optic nerve dysfunction in ODD patients.

Patients and Methods

The study was a prospective observational study approved by the scientific ethics committee of the Capital Region, Denmark (H-4-2013-040).

Patient Selection

Patients diagnosed with ODD from January 1, 2009, to January 1, 2016, were asked to participate in the study. All patients were seen at the Department of Ophthalmology at Rigshospitalet-Glostrup, Denmark. The patient exclusion criteria were best corrected visual acuity (BCVA) >logMAR 0.2, age <18 years, and presence of systemic disease that could affect optic nerve function. Exclusion criteria for individual eyes were localized eye or optic nerve disease other than ODD (e.g., optic neuritis, glaucoma, etc.) or ODD complications (e.g., drusen-associated anterior ischemic optic neuropathy, central retinal artery, vein occlusion, etc.) that could affect optic nerve function.

Informed consent was obtained from the subjects after explanation of the nature and possible consequences of the study. All procedures adhered to the tenets of Declaration of Helsinki.

Data Acquisition

All examinations were performed by a single examiner (LM). All included participants were asked about medication use as well as ophthalmic and medical history. Best corrected visual acuity was determined using Early Treatment Diabetic Retinopathy Study (ETDRS) charts (4-meter original series; Precision-Vision, La Salle, IL, USA). Patients were examined using slit lamp biomicroscopy and intraocular pressure was measured by applanation tonometry. Spectral domain EDI-OCT (Spectralis HRA+OCT; Heidelberg Engineering, Heidelberg, Germany) was performed using the following protocol: (1) dense optic nerve head scan for identification and quantification of ODD with EDI-OCT in both vertical and horizontal directions with 30 μm between each B-scan (97 scans), averaging 30 B-scans; (2) peripapillary evaluation of RNFL thickness with a 12° circumferential scan; and (3) macula overview in vertical direction with 240 μm between each B-scan for evaluation of macular GCL thickness. All scans were performed in high resolution with averaging of B-scans using the built-in eye tracking feature. Patients were dilated with 2.5% phenylephrine before OCT acquisition.

Recording and analysis of mfVEP data was performed as previously described.[14] Briefly, patients were stimulated in a viewing distance of 30 cm to a screen (22-inch, high-resolution LCD display, 90% brightness and 65% contrast; Hitachi, Ltd., Tokyo, Japan) containing a cortically scaled 56-segment dartboard pattern with 16 checks alternating between black and white in each segment according to a pseudorandom sequence. The test was performed nondilated with optimal refraction. The central 1° of the screen contained an interactive fixation area. We recorded the mfVEP using a commercial system (VisionSearch1; VisionSearch, Sydney, Australia) in a vertical (a positive electrode 2.5 cm above inion and a negative reference electrode 4.5 cm below inion) and horizontal (a positive electrode 4 cm left of inion and a negative reference electrode 4 cm right of the inion) channel. The data sampling rate was 600 Hz with a recording length of 832 ms. We obtained the mfVEP responses by correlating visual stimuli with recorded electrical potentials.

Visual field analysis was obtained using automated perimetry (Octopus, Haag-Streit, Switzerland) with a 30-2 test pattern.

Data Analysis

Specialized software (Heidelberg Eye Explorer, version 1.9.10.0; Heidelberg Engineering) was used to assess all OCT parameters. Integrated automated segmentation software was used in all scans and manually verified and adjusted. Macular GCL was measured in a circular area of 3 to 6 mm from the foveola. Global peripapillary RNFL thickness was measured centering the scan at the optic disc. Scleral canal size was manually measured as the mean of the largest vertical and horizontal opening of Bruch's membrane. The dense optic nerve head scan was exported from the integrated software and was manually analyzed using a medical image segmentation tool (ITK-Snap; ITK-Snap ver. 3.2.0, www.itksnap.org; in the public domain).[15] The volume of ODD was calculated by manual segmentation of ODD in 97 B-scans per eye. Each ODD was localized and individually segmented in each B-scan to calculate ODD volumes. The definition of ODD using OCT was based on previous studies[12,16–19] and defined as hyporeflective structures with a full or partial hyperreflective margin. See Supplementary Movie S1 for a 3D view of a segmented optic nerve head. To quantify the vertical anatomic location of each ODD, an automated graph-based segmentation of Bruch's membrane[20] at the margin in each B-scan was performed with computing software (MATLAB; The MathWorks, Inc., Natick, MA, USA). A reference surface relative to Bruch's membrane was defined from these landmarks (Fig. 1). The height difference from the center of mass of each ODD to the reference surface was thereafter calculated with negative values referring to localization above the reference surface and positive values referring to localization below the reference surface. The anatomic vertical location of each ODD was multiplied by the volume fraction of the same ODD relative to the total ODD volume in each patient to quantify the anatomic vertical center of weighted ODD mass. This means that a large deep ODD would have a greater impact on the vertical anatomic center of weighted ODD mass than a small superficial ODD, and thereby result in a deeper overall localization. On the other hand, if the superficial ODD was larger, the weighted center of mass would move toward a more superficial localization.

The agreement of ODD volume was assessed in 10 randomly selected patients with intraobserver variability using Bland-Altman plots. Intraobserver agreement in ODD volume assessment revealed a mean difference between measurements of 0.027 mm^3 (SD ± 0.035), representing 9% of the mean ODD volume. Bland-Altman plots showed acceptable variability, no trend and limits of agreement between –0.062 and 0.099 mm^3.

Responses of MfVEP were obtained by correlating visual stimuli with recorded electrical potentials using integrated software (Terra, version 1.6; VisionSearch, Sydney, Australia). Peak-to-peak (P2P) amplitude and monocular latency (second peak) was obtained using the integrated software after manual validation of the responses. Signal-to-noise ratio (SNR) amplitude was calculated in a computing environment (The MathWorks, Inc.) as described in previous work.[14]

Statistical Analysis

Statistical analyses were performed using commercial software (SAS, version 9.1; SAS Institute, Cary, NC, USA). To avoid statistical bias, only one eye was included for each patient. The

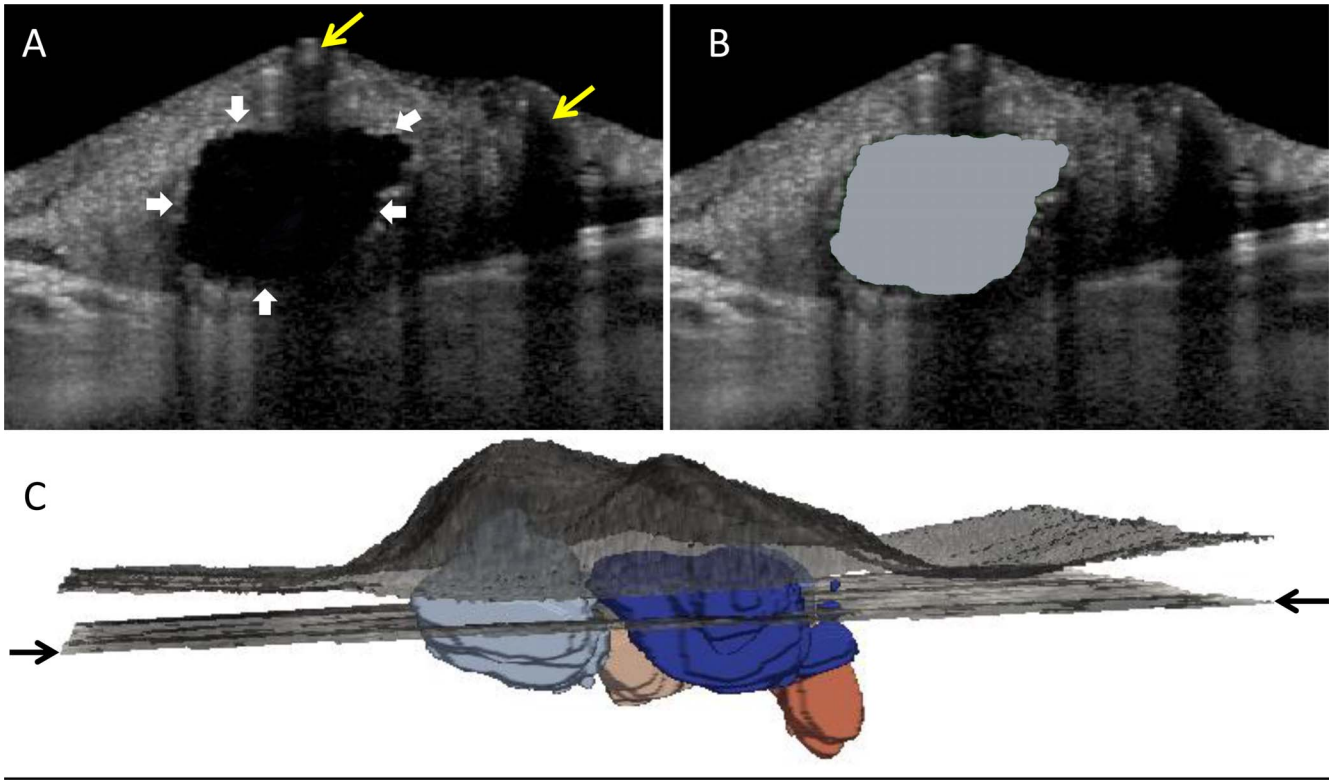

FIGURE 1. Visualization of the process going from EDI-OCT scans to 3D volume of ODD. (**A**) Single EDI-OCT B-scan with a prominent ODD (*white arrowheads*). *Yellow arrows* represent vessels. (**B**) We performed 2D segmentation of ODD (*painted area*) in each B-scan. (**C**) A total of 97 segmented B-scans created the final 3D segmentation. To quantify the vertical anatomic location of each ODD a reference surface relative to Bruch's membrane was defined using an automated graph based segmentation of Bruch's membrane (*black arrow*). Four individual ODD are seen in different colors.

eye with worst MD on automated perimetry was used in patients with bilateral ODD.

Mean and standard deviations or median and interquartile ranges (skewed distributions) were reported for continuous variables. Student's *t*-test or Wilcoxon signed-rank test (skewed distribution) was used to compare patients with visible and buried ODD. We used χ^2 or Fisher's exact tests (expected count <5) for categorical data.

The assumptions of linearity, homoscedasticity, and normal distribution of residuals were tested when performing multiple regressions. The contribution of each predictor in the multiple regression analysis was found by assessing standardized parameter estimates (the change in *Y*, measured in units of its standard deviation, associated with a 1 standard deviation change in *X*). The assumptions of linearity, homoscedasticity, related pairs, and normality of variables were tested when performing correlation analysis. Adjustment for multiple testing in the correlation analyses was performed using the Holm-Bonferroni method. The predetermined level of statistical significance for the comparisons was $P \leq 0.05$.

RESULTS

We included 37 patients (30 women and 7 men) in this study. All included patients were Caucasian. Bilateral ODD were found in 95% of the patients. All eyes with ODD had one or more hyporeflective structures with a full or partial hyperreflective margin using OCT. Differences in clinical, mfVEP, and EDI-OCT findings were compared between patients with visible (visible by ophthalmoscopy) and buried (only visible by EDI-OCT) ODD (Table 1). Patient with buried ODD were significantly younger (median age: 21 years) than patients with visible ODD (median age: 33 years; $P = 0.015$). Significantly thinner peripapillary RNFL thickness and macular GCL thickness (3–6 mm from fovea) were found in patients with visible ODD ($P < 0.001$, $P = 0.002$). A tendency toward larger scleral canal size in patients with visible ODD was found ($P = 0.05$). A worse MD was found in patients with visible ODD (–4.3 dB) when compared to patients with buried ODD (–1.9 dB; $P = 0.025$). The quantitative measure of anatomic location was significantly different between the two groups with the center of weighted ODD mass being 172 μm below the reference level in patients with visible ODD and 306 μm below the reference level in patients with buried ODD ($P = 0.046$). Volume of ODD was larger in patients with visible ODD (0.29 mm^3) than in patients with buried ODD (0.01 mm^3; $P = 0.002$).

A multiple linear regression was calculated to predict MD based on ODD volume, visibility by ophthalmoscopy, anatomic ODD location, and age. A significant regression equation was found ($R^2 = 0.52$, $P < 0.0001$). Larger ODD volume was associated with worse MD ($P < 0.0001$). For every 1 mm^3 increase in ODD volume, the MD decreased by 18.1 dB (CI 95% –25.6 to –10.7 dB). Anatomic ODD location, age, and visibility by ophthalmoscopy were not found significantly associated with MD when adjusted for the other variables. When looking at standardized parameter estimates, ODD volume had a higher effect on MD when compared to weighted ODD location. Figure 2 illustrates the ODD segmentation, en face overview, and corresponding visual field and RNFL thickness map in three selected patients.

Another multiple linear regression was performed to estimate the relative effect of RNFL and macular GCL thickness on MD. A significant regression equation was found ($R^2 = 0.58$,

Table 1. Differences in Clinical, mfVEP, and EDI-OCT Findings in Patients With Visible and Buried ODD

Variable	Visible ODD ($n = 32$)	Buried ODD ($n = 5$)	*P* Values
Female sex, *n*	26	4	1.0*
Age, y	33 (26)	21 (1)	0.015†
Refractive error, D	−0.75 ± 3.1	0.95 ± 2.8	0.28‡
IOP, mm Hg (applanation tonometry)	13 (3)	13 (2)	0.98†
BCVA, (ETDRS, letters)	88 (6)	87 (1)	0.79†
Ishihara	16/16	16/16	0.44†
RAPD	8	0	0.56*
MD, dB	−4.5 (10.3)	-1.9 (2.6)	0.025†
Peak-to-peak mfVEP amplitude, nV	122 ± 55	131 ± 48	0.74‡
Signal-to-noise ratio mfVEP amplitude	3.8 ± 1.1	3.3 ± 0.6	0.29‡
Second peak mfVEP latency, ms	154±9	153 ± 2	0.81‡
Peripapillary RNFL thickness, μm	66.6 ± 20	101.4 ± 6.8	<0.001‡
Retinal macular thickness, μm	277.8 ± 20.7	279.2 ± 10.6	0.83‡
Macular GCL thickness 3–6 mm, μm	29.5 ± 5.8	36.4 ± 3.0	0.002‡
Scleral canal diameter, μm	1631 (230)	1477 (114)	0.05†
ODD volume, mm^3	0.29 (0.41)	0.01 (0.02)	0.002†
Mean anatomic location below reference level, μm	49 (211)	295 (114)	0.007†

D, diopter; IOP, intraocular pressure; RAPD, relative afferent pupillary defect.
* χ^2 test.
† Wilcoxon rank sum test.
‡ Student's *t*-test.

$P < 0.0001$). Worse MD was significantly associated only with GCL thickness ($P = 0.025$) when adjusted for the other variable. Mean deviation increased by 0.65 dB (CI 95% 0.08–1.2 dB) for every 1 μm increase in GCL thickness. When looking at standardized parameter estimates, GCL thickness had a higher effect on MD when compared to RNFL thickness.

Table 2 summarizes the correlation between anatomic and functional markers of optic nerve dysfunction. Macular GCL thickness had the highest degree of correlation when compared to MD ($\rho = 0.76$, $P < 0.0001$), while macular GCL thickness and peripapillary RNFL thickness were comparable when looking at mfVEP parameters. The unadjusted correlation coefficient for the correlation between ODD volume and MD was −0.66 (Fig. 3).

Discussion

Our study is, to the best of our knowledge, the first to quantitatively assess both the ODD volume and anatomic location of ODD. Using visibility by ophthalmoscopy to classify ODD in superficial or buried might be obsolete due to technical advances in imaging techniques. We therefore calculated ODD volume and anatomic location quantitatively and applied it in a multivariate model for a better understanding of their relative contribution to optic nerve dysfunction.

We found that a larger ODD volume resulted in worse MD when adjusted for age, visibility by slit lamp, and anatomic location. Other studies have quantitatively assessed ODD size,[11,12] and similar results were found in a recent case-series including five patients,[12] where an excellent correlation between ODD volume and MD using automated perimetry was found. We suspect the increasing optic nerve dysfunction caused by larger ODD volume might be a result of either direct compression of adjacent ganglion cell axons, leading to ganglion cell death or secondary to compromised vascular flow.[21]

No association between weighted anatomic ODD location and MD was found in the current study. This is interesting as several studies have found worse MD in patients with ophthalmoscopically visible ODD.[8,22,23] Other studies have further found more abnormal visual fields in patients with visible ODD when compared to patients with buried ODD.[24–26] The results from this study suggest that age, ODD volume, and ODD location all contribute to ODD visibility. This means that equating ODD visibility on ophthalmoscopy with superficial anatomic ODD location only, incorrectly leads one to believe that there is an association between superficial anatomic ODD location and worse MD. Our findings suggest that solely larger ODD volume, and not a more superficial ODD location, results in higher degrees of visual field defects.

Based on our finding that visibility by ophthalmoscopy did not have an effect on MD when adjusted for age, ODD volume and ODD location, we argue that the classification using ODD visibility by ophthalmoscopy is not ideal to estimate optic nerve dysfunction. Furthermore, the term "superficial", often used in the classification, is misleading as several factors, such as age and ODD volume, influence the visibility. In this regard, the term "visible" ODD might therefore be more appropriate to use than superficial ODD.

We found differences in age, MD, RNFL, and GCL thickness that are supported by several studies when using the classification of ODD as visible or buried.[8–11,23,27] Our results of the multivariate analysis suggest that GCL thickness is a better anatomic correlate to optic nerve dysfunction in ODD patients than RNFL thickness. While the macular GCL thickness has not been explored extensively in ODD literature, macular ganglion cell–inner plexiform layer thickness has proven to be a predictor of early glaucoma with the same sensitivity as RNFL thickness.[28,29] It has even been suggested that individually segmented GCL thickness could be a better predictor for the presence of preperimetric glaucoma than RNFL thickness.[30]

Conflicting results have been published about the role of scleral canal size in ODD etiology.[31–34] A larger scleral canal in patients with superficial ODD has been previously reported,[33,34] and in this study, the same tendency was found. In unpublished data (Malmqvist L, unpublished poster presentation, 2016), we have found smaller scleral canal in ODD children when compared to healthy children and we therefore suggest the finding of this study is due to a displacement of Bruch's membrane caused by distending ODD. This was originally proposed as an alternative explanation for similar findings in a study by Floyd et al.[34] Our proportion of patients

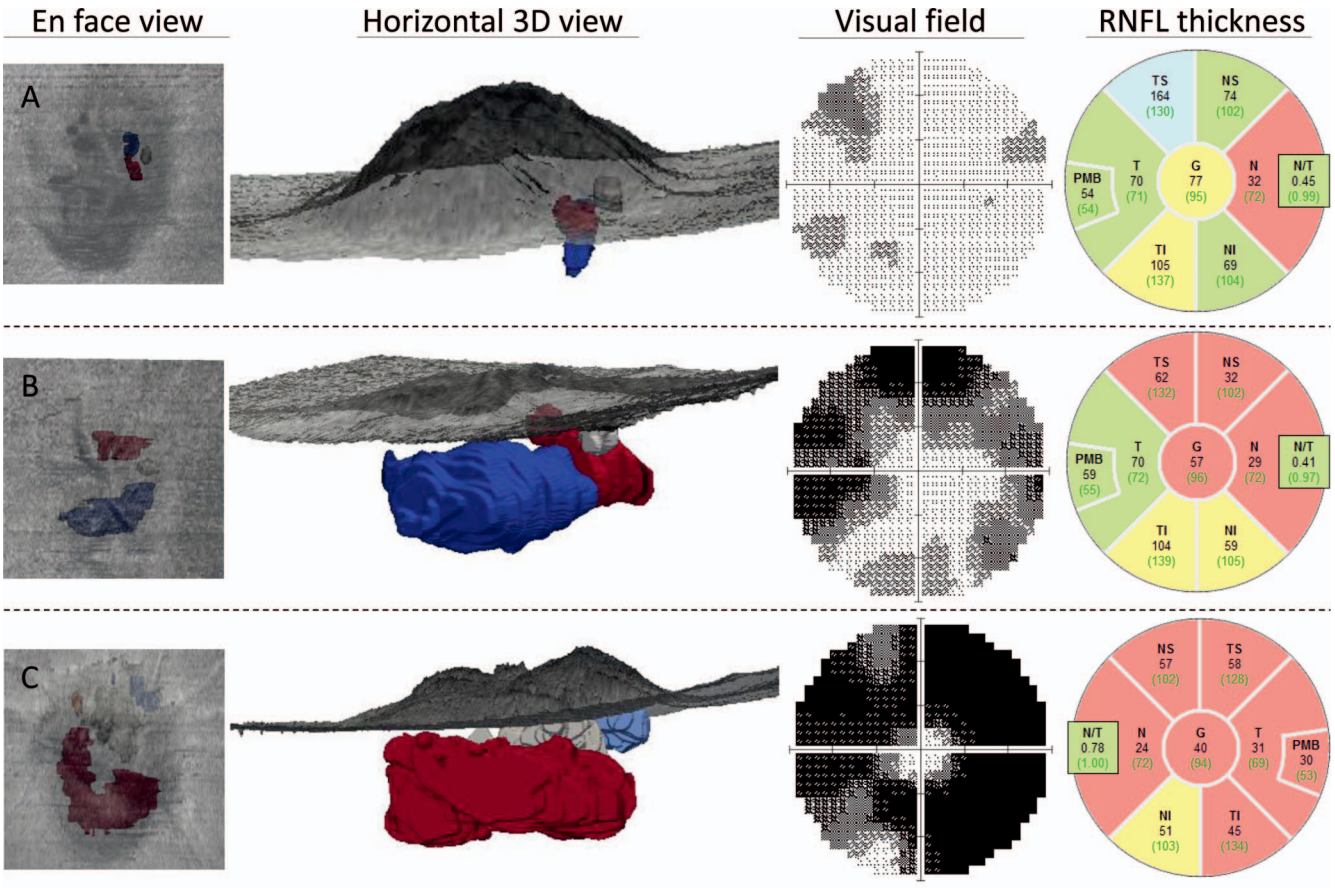

Figure 2. En face view and horizontal 3D view of optic nerve head and segmented ODD, as well as corresponding visual fields and RNFL thickness map in three different patients. Different colors symbolize the individual drusen. Colors in the RNFL thickness map indicate if the thickness in different regions is within or outside the statistical limits of normality: *green*, normal; *yellow*, borderline below normal limits; *red*, below normal limits; *blue*, borderline above normal limits. (**A**) Right eye of a patient with total ODD volume of 0.07 mm^3. Visual field testing revealed a near-normal mean deviation of −2.9 dB and global RNFL thickness was decreased to 77 μm. (**B**) Right eye of a patient with total ODD volume of 0.23 mm^3. Visual field testing revealed a mean deviation of −12.3 dB and global RNFL thickness was decreased to 57 μm. (**C**) Left eye of a patient with total ODD volume of 0.69 mm^3. Visual field testing revealed a mean deviation of −24.3 dB and global RNFL thickness was decreased to 40 μm.

with bilateral ODD (95%) is the highest reported in the literature.

Most studies have reported bilateral ODD in 62% to 76% of patients.[8,11,35,36] By using EDI-OCT in our study, we were able to diagnose eyes with small and deeply buried ODD overlooked by ophthalmoscopy, autofluorescence, B-scan ultrasound, and even conventional spectral-domain OCT. Based on these results, we propose that bilateral ODD are more common than previously believed.

Table 2. Correlation Coefficients for Correlations Between Anatomic and Functional Markers of Optic Nerve Dysfunction

Variable	Automated Perimetry MD	Multifocal Visual Evoked Potentials		
		P2P	SNR	Latency
ODD volume	−0.66*	−0.43	−0.22	0.28
RNFL thickness	0.72*	0.51*	0.43*	−0.48*
GCL thickness	0.76*	0.56*	0.48*	−0.48*

Pearson's correlation coefficient between anatomic and functional markers of optic nerve dysfunction.

* Holm-Bonferroni adjusted significant ($P < 0.05$). Latency was measured as second peak latency. Global RNFL thickness was measured peripapillary. Thickness of GCL was measured as the mean of a 3 to 6 mm ring around the fovea.

In this study, we included mfVEP amplitude and latency as an objective measure of optic nerve function as previous studies have found significantly decreased amplitude and latency delays in patients with optic disc drusen when compared to control subjects.[37,38] Hence an association between ODD volume and mfVEP parameters was expected. Parameters of mfVEP were significantly correlated with RNFL and GCL thickness, but not with ODD volume. That mfVEP amplitude was not correlated with ODD volume is likely a result of the high intersubject variability[14] and in this case, we assume that the variability was too high to describe the more subtle changes in optic nerve dysfunction when only comparing ODD patients.

The major limitation of the study was the use of multiple regression analysis with the limited amount of patients. By using the covariate "visibility by ophthalmoscopy," including only five eyes with buried ODD, the estimation was not strong. The fact that we, in multiple regression analyses, did not find an association between RNFL thickness and MD, can be ascribed to multicollinearity, as RNFL and GCL thickness were correlated. In this study, transverse magnification was not measured to account for the effect of optical magnification. However, the mean spherical equivalent refraction was not significantly different between patients with visible and buried ODD. In this study, we exclusively measured the volume of ODD defined as hyporeflective structures with a full or partial

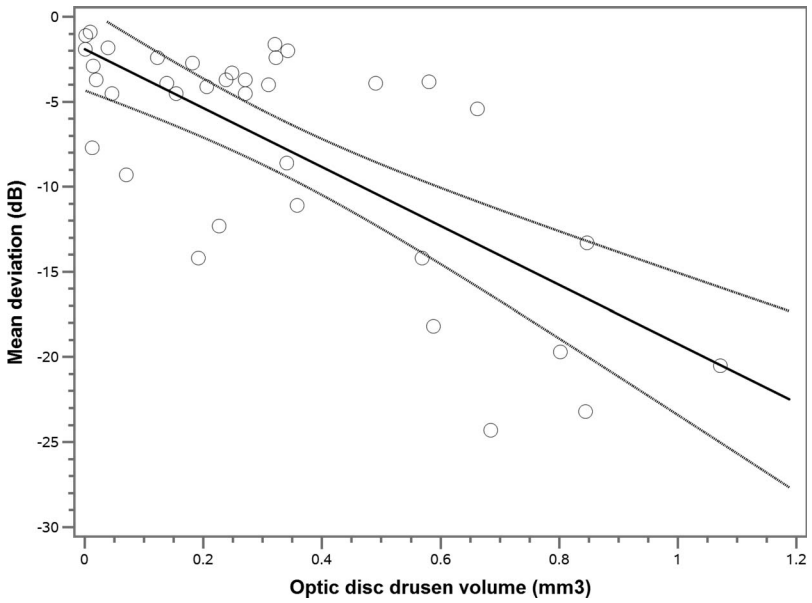

FIGURE 3. Unadjusted total ODD volume as a function of automated perimetric MD; $\rho = -0.66$. *Black line* represents regression line. *Gray line* represents 95% confidence limits.

hyperreflective margin. However, other studies have reported ODD as either hyperreflective, granular, or hyporeflective when using OCT.[11,39] The conflicting descriptions of ODD morphology are a limitation in this as well as other ODD studies, and should be addresses in future research.

In conclusion, this study suggests that ODD volume is significantly associated with optic nerve dysfunction. Even though a worse MD is often found in patients with visible ODD, a more superficial anatomic ODD location is not necessarily associated with worse MD. The current classification using visibility by ophthalmoscopy is an unspecific marker of optic nerve dysfunction compared to quantitative measurements of ODD volume using EDI-OCT.

Acknowledgments

Supported by Fight for Sight, Denmark, and Synoptik-Fonden.

Disclosure: **L. Malmqvist**, None; **A.-S.W. Lindberg**, None; **V.A. Dahl**, None; **T.M. Jørgensen**, None; **S. Hamann**, None

References

1. Spencer WH. Drusen of the optic disk and aberrant axoplasmic transport. The XXXIV Edward Jackson memorial lecture. *Am J Ophthalmol*. 1978;85:1–12.
2. Friedman AH, Gartner S, Modi SS. Drusen of the optic disc. A retrospective study in cadaver eyes. *Br J Ophthalmol*. 1975; 59:413–421.
3. Lee AG, Zimmerman MB. The rate of visual field loss in optic nerve head drusen. *Am J Ophthalmol*. 2005;139:1062–1066.
4. Petersen HP. Colloid bodies with defects in the field of vision. *Acta Ophthalmologica*. 1957;35:243–272.
5. Khan MA, Forman AR. Legal blindness from severe optic nerve head drusen. *JAMA Ophthalmol*. 2016;134:e153660.
6. Knight CL, Hoyt WF. Monocular blindness from drusen of the optic disk. *Am J Ophthalmol*. 1972;73:890–892.
7. Auw-Haedrich C, Staubach F, Witschel H. *Optic disk drusen*. *Surv Ophthalmol*. 2002;47:515–532.
8. Malmqvist L, Wegener M, Sander BA, Hamann S. Peripapillary retinal nerve fiber layer thickness corresponds to drusen location and extent of visual field defects in superficial and buried optic disc drusen. *J Neuroophthalmol*. 2016;36:41–45.
9. Traber GL, Weber KP, Sabah M, Keane PA, Plant GT. Enhanced depth imaging optical coherence tomography of optic nerve head drusen: a comparison of cases with and without visual field loss. *Ophthalmology*. 2017;124:66–73.
10. Mistlberger A, Sitte S, Hommer A, et al. Scanning laser polarimetry (SLP) for optic nerve head drusen. *Int Ophthalmol*. 2001;23:233–237.
11. Lee KM, Woo SJ, Hwang JM. Morphologic characteristics of optic nerve head drusen on spectral-domain optical coherence tomography. *Am J Ophthalmol*. 2013;155:1139–1147.e1131.
12. Yi K, Mujat M, Sun W, et al. Imaging of optic nerve head drusen: improvements with spectral domain optical coherence tomography. *J Glaucoma*. 2009;18:373–378.
13. Lee KM, Woo SJ, Hwang JM. Morphologic characteristics of optic nerve head drusen on spectral-domain optical coherence tomography. *Am J Ophthalmol*. 2013;155:1139–1147.
14. Malmqvist L, De Santiago L, Fraser C, Klistorner A, Hamann S. Exploring the methods of data analysis in multifocal visual evoked potentials. *Doc Ophthalmol*. 2016;133:41–48.
15. Yushkevich PA, Piven J, Hazlett HC, et al. User-guided 3D active contour segmentation of anatomical structures: significantly improved efficiency and reliability. *Neuroimage*. 2006; 31:1116–1128.
16. Merchant KY, Su D, Park SC, et al. Enhanced depth imaging optical coherence tomography of optic nerve head drusen. *Ophthalmology*. 2013;120:1409–1414.
17. Sato T, Mrejen S, Spaide RF. Multimodal imaging of optic disc drusen. *Am J Ophthalmol*. 2013;156:275–282.e1.
18. Ghassibi MP, Chien JL, Abumasmah RK, Liebmann JM, Ritch R, Park SC. Optic nerve head drusen prevalence and associated factors in clinically normal subjects measured using optical coherence tomography. *Ophthalmology*. 2017;124:320–325.
19. Slotnick S, Sherman J. Buried disc drusen have hypo-reflective appearance on SD-OCT. *Optom Vis Sci*. 2012;89:E704–E708.
20. Li K, Wu X, Chen DZ, Sonka M. Optimal surface segmentation in volumetric images–a graph-theoretic approach. *IEEE Trans Pattern Anal Mach Intell*. 2006;28:119–134.

21. Abegao Pinto L, Vandewalle E, Marques-Neves C, Stalmans I. Visual field loss in optic disc drusen patients correlates with central retinal artery blood velocity patterns. *Acta Ophthalmol*. 2014;92:e286–e291.
22. Gili P, Flores-Rodriguez P, Martin-Rios MD, Carrasco Font C. Anatomical and functional impairment of the nerve fiber layer in patients with optic nerve head drusen. *Graefes Arch Clin Exp Ophthalmol*. 2013;251:2421–2428.
23. Roh S, Noecker RJ, Schuman JS, Hedges TR III, Weiter JJ, Mattox C. Effect of optic nerve head drusen on nerve fiber layer thickness. *Ophthalmology*. 1998;105:878–885.
24. Mustonen E. Pseudopapilloedema with and without verified optic disc drusen. A clinical analysis II: visual fields. *Acta Ophthalmologica*. 1983;61:1057–1066.
25. Wilkins JM, Pomeranz HD. Visual manifestations of visible and buried optic disc drusen. *J Neuroophthalmol*. 2004;24:125–129.
26. Savino PJ, Glaser JS, Rosenberg MA. A clinical analysis of pseudopapilledema. II. Visual field defects. *Arch Ophthalmol*. 1979;97:71–75.
27. Casado A, Rebolleda G, Guerrero L, et al. Measurement of retinal nerve fiber layer and macular ganglion cell-inner plexiform layer with spectral-domain optical coherence tomography in patients with optic nerve head drusen. *Graefes Arch Clin Exp Ophthalmol*. 2014;252:1653–1660.
28. Rao HL, Zangwill LM, Weinreb RN, Sample PA, Alencar LM, Medeiros FA. Comparison of different spectral domain optical coherence tomography scanning areas for glaucoma diagnosis. *Ophthalmology*. 2010;117:1692–1699, 1699.e1.
29. Nouri-Mahdavi K, Nowroozizadeh S, Nassiri N, et al. Macular ganglion cell/inner plexiform layer measurements by spectral domain optical coherence tomography for detection of early glaucoma and comparison to retinal nerve fiber layer measurements. *Am J Ophthalmol*. 2013;156:1297–1307.e2.
30. Nakano N, Hangai M, Nakanishi H, et al. Macular ganglion cell layer imaging in preperimetric glaucoma with speckle noise-reduced spectral domain optical coherence tomography. *Ophthalmology*. 2011;118:2414–2426.
31. Jonas JB, Gusek GC, Guggenmoos-Holzmann I, Naumann GO. Optic nerve head drusen associated with abnormally small optic discs. *Int Ophthalmol*. 1987;11:79–82.
32. Mullie MA, Sanders MD. Scleral canal size and optic nerve head drusen. *Am J Ophthalmol*. 1985;99:356–359.
33. Flores-Rodriguez P, Gili P, Martin-Rios MD, Grifol-Clar E. Comparison of optic area measurement using fundus photography and optical coherence tomography between optic nerve head drusen and control subjects. *Ophthalmic Physiol Opt*. 2013;33:164–171.
34. Floyd MS, Katz BJ, Digre KB. Measurement of the scleral canal using optical coherence tomography in patients with optic nerve drusen. *Am J Ophthalmol*. 2005;139:664–669.
35. Boldt HC, Byrne SF, DiBernardo C. Echographic evaluation of optic disc drusen. *J Clin Neuroophthalmol*. 1991;11:85–91.
36. Lorentzen SE. Drusen of the optic disk. A clinical and genetic study. *Acta Ophthalmologica*. 1966(suppl 90):91–180.
37. Grippo TM, Ezon I, Kanadani FN, et al. The effects of optic disc drusen on the latency of the pattern-reversal checkerboard and multifocal visual evoked potentials. *Invest Ophthalmol Vis Sci*. 2009;50:4199–4204.
38. Malmqvist L, de Santiago L, Boquete L, Hamann S. Multifocal visual evoked potentials for quantifying optic nerve dysfunction in patients with optic disc drusen [published online ahead of print January 31, 2017]. *Acta Ophthalmol*. doi:10.1111/aos.13347.
39. Traber GL, Weber KP, Sabah M, Keane PA, Plant GT. Enhanced depth imaging optical coherence tomography of optic nerve head drusen: a comparison of cases with and without visual field loss. *Ophthalmology*. 2017;124:66–73.

Investigative Ophthalmology & Visual Science